Boletim da Sociedade Astronômica Brasileira, **33**, no. 1, 144-148

The efficiency analysis of high-eccentricity mechanisms for the production of hot Jupiter candidates

H. Garzón[1], Adrián Rodríguez[1], & G. C. de Elía[2,3]

[1] Observatório do Valongo, Universidade Federal do Rio de Janeiro, Ladeira do Pedro Antônio 43, 20080-090, Rio de Janeiro, Brazil
e-mail: adrian@astro.ufrj.br
[2] Instituto de Astrofísica de La Plata, CCT La Plata-CONICET-UNLP, Paseo del Bosque S/N (1900), La Plata, Argentina
[3] Facultad de Ciencias Astronómicas y Geofísicas, Universidad Nacional de La Plata, Paseo del Bosque S/N (1900), La Plata, Argentina

Abstract. Hot Jupiters (HJs) are giant planets with orbital periods of the order of a few days with semimajor axis within ~0.1 au. Several theories have been invoked in order to explain the origin of this type of planets, one of them being the high-eccentricity migration. This migration can occur through different high-eccentricity mechanisms. Our investigation focused on six different kinds of high-eccentricity mechanisms, namely, the planet–planet scattering, coplanar, Kozai-Lidov, secular chaos, E1 and E2 mechanisms. We investigated the efficiency of these mechanisms for the production of HJ candidates, considering a large set of numerical simulations of the exact equations of motion in the context of the N-body problem. In particular, we analyzed the sensitivity of our results to the initial number of planets, the initial semimajor axis of the innermost planetary orbit, the initial configuration of planetary masses, and to the inclusion of general relativity effects. We found that the E1 mechanism is the most efficient in producing HJ candidates both in simulations with and without the contribution of general relativity, followed by the Kozai-Lidov and E2 mechanisms. Our results also revealed that, except for the initial equal planetary mass configuration, the E1 mechanism was notably efficient in the other initial planetary mass configurations considered in this work. The present work has allowed us to improve our understanding about the dynamical evolution of systems that undergo strong instability events between gaseous giant planets, exploring in detail the production of HJ candidates via high-eccentricity mechanisms.

Resumo. Júpiteres Quentes (JQs) são planetas gigantes com períodos orbitais da ordem de alguns dias com semi-eixo maior de até 0,1 UA. Diversas teorias têm sido invocadas para explicar a origem desse tipo de planetas, sendo uma delas a migração de alta excentricidade. Essa migração pode ocorrer por meio de diferentes mecanismos de alta excentricidade. Nossa investigação se concentrou em seis tipos diferentes de mecanismos de alta excentricidade, a saber, o espalhamento planeta- planeta, coplanar, Lidov-Kozai, caos secular, mecanismos E1 e E2. Nós investigamos a eficiência desses mecanismos para a produção de candidatos a JQ, considerando um grande conjunto de simulações numéricas das equações exatas do movimento, no contexto do problema geral dos N corpos. Em particular, analisamos a sensibilidade de nossos resultados em relação ao número inicial de planetas, o semi-eixo maior inicial da órbita planetária mais interna, a configuração inicial das massas planetárias e a inclusão dos efeitos da relatividade geral. Descobrimos que o mecanismo E1 é o mais eficiente na produção de candidatos a JQ tanto em simulações com e sem a contribuição da relatividade geral, seguido pelos mecanismos Lidov-Kozai e E2. Nossos resultados também revelaram que, exceto para a configuração inicial na qual todos os planetas possuem a mesma massa, o mecanismo E1 foi notavelmente eficiente nas outras configurações iniciais de massa planetária consideradas neste trabalho. O presente trabalho nos permitiu aprimorar nosso entendimento sobre a evolução dinâmica de sistemas que sofrem fortes eventos de instabilidade inicial entre planetas gigantes gasosos, explorando em detalhe a produção de candidatos a JQ via mecanismos de alta excentricidade.

Keywords. Celestial mechanics – Planets and satellites: dynamical evolution and stability – Methods: numerical

1. Introduction

Different theories have been proposed to explain the origins of hot Jupiters (HJs). One of them is in-situ formation (Bodenheimer et al. 2000; Batygin et al. 2016; Boley et al. 2016; Bailey & Batygin 2018; Poon et al. 2021). In this theory, HJ originates without requiring a significant orbital migration process and may be accompanied by nearby planets (e.g. Boley et al. 2016; Poon et al. 2021). In the case of disk migration theory (see, e.g. Lin et al. 1996; Fogg & Nelson 2005; Mandell et al. 2007; Coleman & Nelson 2016; Heller 2019), HJ is produced through gravitational and dissipative interactions between the giant planet and the protoplanetary disk, and may also be accompanied by nearby planets but with the trend to be resonant companions (e.g. Lee & Peale 2002; Raymond et al. 2006; Mandell et al. 2007; Ogihara et al. 2014). In contrast, high-eccentricity migration theory has difficulty producing HJs with nearby companions (see, e.g. Marzari & Weidenschilling 2002; Nagasawa et al. 2008; Wu & Lithwick 2011; Naoz et al. 2011; Petrovich 2015; Wang et al. 2017; Yi-Han et al. 2020). This is due to the dynamic instabilities generated in the multiplanetary system during the eccentricity excitation phase, where the giant planet gets a highly eccentric orbit (usually $e \gtrsim 0.9$) due to gravitational interaction with neighboring giant planets or substellar/stellar companion as well as in the decay phase of the semimajor axis, in which the giant planet dissipates its orbital energy during the periastron passage due to the tidal interaction with the host star (Ivanov & Papaloizou 2004).

In high-eccentricity migration, there are several proposed dynamical mechanisms that have the ability to excite the giant planet's eccentricity to high values and, therefore, reduce its orbital angular momentum. Among the proposed dynamical mechanisms are planet-planet scattering, which has the ability to modify the semimajor axes of planets from a series of multiple close encounters that can lead to collisions, impacts with the host star or ejection of some of them (e.g. Rasio & Ford 1996; Marzari & Weidenschilling 2002;

Nagasawa et al. 2008; Beaugé & Nesvorný 2012; Zanardi et al. 2017; Anderson et al. 2020), and those that are of secular interactions, where the orbital energies of the planets remain constant as long as dissipative interactions are not taken into account, which includes planet-planet and planet-substellar/star companion Kozai-Lidov (e.g. Naoz et al. 2011, 2012; Vick et al. 2019), coplanar (Petrovich 2015; Xue et al. 2017), secular chaos (Wu & Lithwick 2011; Teyssandier et al. 2019), E1 and E2 mechanisms (Wang et al. 2017).

The aim of our study is to obtain a broader and more detailed description of the efficiency of each high-eccentricity mechanism in the activation of the HJ production process, including the contribution of general relativity (GR) effects and different initial planetary mass configurations. The analysis is made by solving the numerical simulation of the exact equations of motion, in the context of general N-body problem. Several initial conditions are considered, changing the initial mass and number of planets, the semimajor axis of the inner planet and the location of the other planets in the system. Our study has its motivation in the study of Wang et al. (2017) who also analyzed the efficiency of each high-eccentricity mechanism in the production of HJ candidates but without the contribution of GR and realistic initial planetary mass configurations, that is, unequal masses.

In Section 2 presents the description of the methodology including numerical model and initial conditions, selection criteria as HJ candidate and procedure to identify the high-eccentricity mechanism. Section 3 contains our statistical results about efficiencies of high-eccentricity mechanisms in the production of HJ candidates and its dependence with respect the initial planetary mass configurations. The conclusions can be found in Section 4.

2. Methodology

2.1. Numerical model and initial conditions

Our numerical model included multi-planet systems composed initially of Cold Jupiters (CJs) with densities equal to the Jupiter's mean density ($1.33\,\mathrm{g\ cm^{-3}}$), orbiting a star of $1M_\odot$ and $1R_\odot$. Between three and five CJs were initially located in tightly-packed configurations in order to induce dynamic instability events during their evolutions, which can lead to planet-planet collisions, impacts with the host star, or ejections from the system. To do this, we carried out an extensive set of N-body simulations performed with the Bulirsch-Stoer (BS) algorithm (Press et al. 1992) that has high accuracy using a modified version of the Mercury code, which allows to select the inclusion of GR effects. Those effects were modeled by a perturbation (relativistic perturbation) to the Newtonian acceleration. The Mercury code evolves the orbits of planets allowing collisions between them. Such collisions were treated as perfect mergers, conserving the mass of the interacting bodies. In our N-body simulations, one planet was assumed to be ejected from the system if it reached a distance from the central star greater than 1000 au. In the present study, we carried out 96000 N-body simulations. Of this total, 48000 runs corresponded to numerical experiments with GR effects. For comparison purposes, the numerical experiments of the above set were also carried out without GR effects. This corresponds to the other 48000 runs. These two groups of numerical experiments will be referred to as GR and No-GR simulations in the present work. Finally, each numerical simulation was integrated for 50 Myr.

As initial conditions, we considered multi-planet systems with three, four and five CJs, where the innermost CJ semimajor axis was 1.0 au and 5.0 au. The initial semimajor axis of the others CJs was defined in units of mutual Hill radius ($R_{H,mut}$), so that

$$a_{i+1} - a_i = KR_{H,mut}\ , \tag{1}$$

where

$$R_{H,mut} = \left(\frac{m_i + m_{i+1}}{3M_*}\right)^{1/3} \frac{(a_i + a_{i+1})}{2}\ , \tag{2}$$

being a_i and m_i the semimajor axis and the mass of the ith CJ, respectively, M_* the mass of the host star, and K a dimensionless number that allows to measure the stability limit of multi-planetary systems. We maintain the separation between adjacent CJs in the range established by Wang et al. (2017), that is, $2 \leq K \leq 6$, but with an interval $\Delta K = 0.002$ and not $\Delta K = 0.001$. This change in the value of ΔK was adopted to decrease the run time for each group of simulations because we have considered initial configurations of CJs with different masses in systems that dynamically evolved over 50 Myr.

In the present study, we aimed to focus on realistic mass distributions for the simulated CJs. Thus, based on the statistics of the *NASA Exoplanet Archive* catalog [1], we selected four different groups of initial planetary mass configurations, namely: 1- equal mass, 2- random mass, 3- increasing mass, and 4- decreasing mass. The range of initial planetary masses associated with the random, increasing and decreasing mass configurations was [0.30 - 5.00) M_J. The mass assigned to each CJ in each configuration above has been selected using an uniform distribution. In the case of the equal mass configuration, the initial mass of each CJ was 1.0 M_J.

For each of the four groups of planetary mass configurations, the initial orbits of CJs were assumed to be circular with inclinations i randomly selected in the range $(0°, 2°]$ following an uniform distribution. The initial values of the argument of periastron ω, the longitude of the ascending node Ω, and the mean anomaly M of CJs were randomly chosen between 0° and 360°, also following an uniform distribution.

2.2. Selection criteria as hot Jupiter candidate

In high-eccentricity migration, numerical modeling of the tidal interaction between the planet and the host star is a complex problem since, in general terms, dynamic and equilibrium (or static) tide models must be considered (see, e.g. Ivanov & Papaloizou 2004). In our simulations the tidal effects were not included since we only focused our analysis on the efficiency of each high-eccentricity mechanism in the production of HJ candidates during gravitational planet-planet interactions. To classify a giant planet as HJ candidate, we adopt the selection criteria proposed by Wang et al. (2017). That is, we also just set a boundary of tidal effects in our study and order to quantify it, we use the temporal parameter Δt and the spatial parameter q, which represent a time scale and the pericentric distance of the giant planet, respectively. Hence, a given giant planet will be considered a HJ candidate if, during its orbital evolution, it reaches pericentric distances (q) small enough to stellar tidal dissipation operate efficiently on a time scale (Δt) approximately equal to the orbital decay time scale of the dynamic tide (τ_a). In quantitative terms, a HJ candidate is produced when $q \lesssim 0.05$ au (Rasio & Ford 1996; Marzari & Weidenschilling 2002) and $\Delta t(q \lesssim 0.05\ \mathrm{au}) \approx \tau_a$, where τ_a is given by equation (8) in Nagasawa et al. (2008).

[1] 1167 exoplanets with mass (or minimum mass) in the range [0.3-13.0] M_J. Approximately 83% of them have a mass (or minimum mass) between 0.3-5.0 M_J. Review date 26/August/2021

2.3. Procedure to identify the high-eccentricity mechanism

According with previous works, we identified six different high-eccentricity mechanisms, which are defined by the following criteria:

1. If only one planet survives in the planetary system and reaches a pericentric distance $q \lesssim 0.05$ au, then the mechanism is identified as planet-planet scattering.

2. For planetary systems with more than one surviving planet, if the inner planet reaches a pericentric distance $q \lesssim 0.05$ au and it is dynamically decoupled from the other planets, the mechanism is also identified as planet-planet scattering.

3. If during the dynamic evolution of the planets there are multiple close encounters, leading some of them to reach a pericentric distance $q \lesssim 0.05$ au over a time scale $\Delta t \approx \tau_a$, the planet-planet scattering is the responsible mechanism.

4. In situations with more than one surviving planet, if the phase diagram of e vs $\Delta\varpi$ of the HJ candidate has the characteristics of libration of $\Delta\varpi$ around 0° or 180° as well as situations of circulation of $\Delta\varpi$ with a maximum (or minimum) value of e when $\Delta\varpi$ is around 0° or 180°, but having the mutual inclination $i_{tot} \lesssim 30°$ for a time $\Delta t(q \lesssim 0.05$ au) $\approx \tau_a$, the mechanism is identified as coplanar.

5. If the planet meets the selection criteria as HJ candidate in scenarios where there is a libration of its argument of periastron ω, the Kozai-Lidov is the responsible mechanism.

6. If the semimajor axis of the surviving planets remain constant, the evolution of their eccentricities and inclinations are non-periodic and the phase diagrams e vs ω and e vs $\Delta\varpi$ of the planet that meets the criteria $\Delta t(q \lesssim 0.05$ au) $\approx \tau_a$ does not have the characteristics of Kozai-Lidov and coplanar, respectively, the mechanism is identified as secular chaos.

7. For planetary systems with more than one surviving planet, if the phase diagram of e vs $\Delta\varpi$ of the HJ candidate has typical characteristics of the coplanar mechanism, its argument of periastron ω circulates and the evolution of its inclination includes values higher than 30° reaching the maximum every time its periastron distance reaches the minimum value, the mechanism is identified as E1.

8. The other scenarios with HJ candidates not classified within the situations mentioned above are identified as E2 mechanism.

3. Results

3.1. Efficiencies of high-eccentricity mechanisms in the production of hot Jupiter candidates

Tables 1 and 2 show the statistics obtained from this classification for No-GR and GR simulations, respectively. These tables show the statistics with all initial planetary mass configurations together. The statistics for each initial planetary mass configuration are shown in the Section 3.2.

Based on the results of Tables 1 and 2 we can see that obtained 2134 HJ candidates according to the implemented selection criteria. In our study, 1141 HJ candidates were produced in No-GR scenarios and 993 in GR simulations. This reduction in the number of HJ candidates in the GR scenario may be explained by the fact that GR contributes to reducing the periods and amplitudes of the eccentricity oscillations of the planets in secular evolution as Marzari & Nagasawa (2020) recently showed.

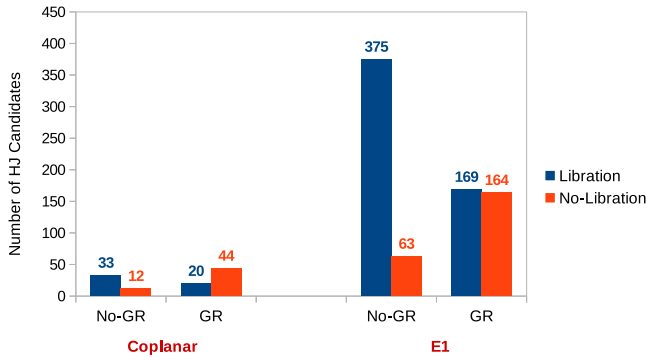

Figure 1. Statistical distribution of the number of HJ candidates produced through coplanar and E1 mechanisms as a function of the characteristics of the phase diagram e vs $\Delta\varpi$ for GR and No-GR scenarios.

As shown in Table 1, our results indicate that the E1 mechanism was the most efficient with 38.39% of the total cases in this scenario, followed by the Kozai-Lidov and E2 mechanisms with 21.74% and 18.58%, respectively. The inclusion of GR showed similarities and differences respect to that obtained in No-GR simulations. Such as Table 2 indicates, the E1 mechanism remained the most efficient in the GR simulations with 33.54%. However, this percentage was less than that derived in the No-GR scenario. If we compare the previous efficiency of the Kozai-Lidov mechanism with the result in Table 1, we can see that GR has the effect of inhibiting the libration of the argument of periastron ω of the HJ candidate. Thus, the efficiency of production of HJ candidates for the Kozai-Lidov mechanism in GR simulations decreased respect to that obtained in No-GR scenario, while coplanar and E2 mechanisms increased their percentages associated with the HJ candidate production. The inclusion of GR also had the effect of decreasing (increasing) the number of HJ candidates with librations (circulations) of $\Delta\varpi$ for the coplanar and E1 mechanisms, which is shown in the statistical distribution of Fig. 1.

We explore how the efficiencies of high-eccentricity mechanisms depend on the initial semimajor axis of the innermost planet (a_1) and initial planet number (N) for GR and No-GR scenarios. Fig. 2 shows the statistical distribution of the number of HJ candidates produced through different high-eccentricity mechanisms as a function of the initial semimajor axis of the innermost planet with and without GR effects. In both scenarios, the results show that between 65% and 68% of HJ candidates were produced with $a_1 = 1.0$ au. According to this, the number of HJ candidates decreases with an increase in the initial value of a_1. For both sets of simulations, E1 remains as the most efficient mechanism in the production of HJ candidates with an increase of a_1. On the other hand, Fig. 3 shows the statistical distribution of the number of HJ candidates produced through different high-eccentricity mechanisms as a function of the initial planet number N for each scenario. Our results indicate that the number of HJ candidates increases with an increase in the initial number of planets both in simulations with and without GR effects.

Table 1. Number of HJ candidates produced (in increasing order) through different high-eccentricity mechanisms for No-GR simulations. The percentages were calculated with respect to the total number of HJ candidates produced in this No-GR scenario.

Coplanar	Secular Chaos	Scattering	E2	Kozai-Lidov	E1
45	73	125	212	248	438
3.94%	6.40%	10.95%	18.58%	21.74%	38.39%

Table 2. Number of HJ candidates produced (in increasing order) through different high-eccentricity mechanisms for GR simulations. The percentages were calculated with respect to the total number of HJ candidates produced in this GR scenario.

Coplanar	Secular Chaos	Scattering	Kozai-Lidov	E2	E1
64	68	139	161	228	333
6.44%	6.85%	14.0%	16.21%	22.96%	33.54%

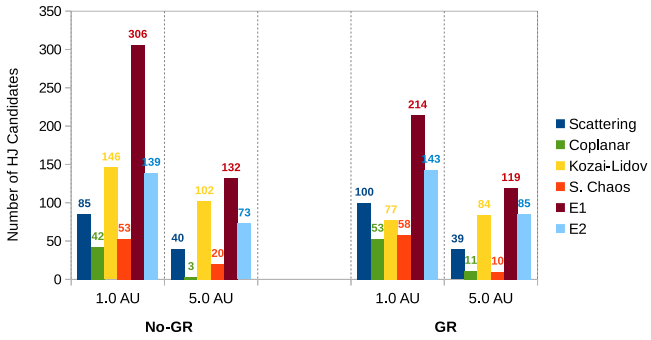

Figure 2. Statistical distribution of the number of HJ candidates produced through different high-eccentricity mechanisms as a function of the initial semimajor axis of the innermost planet for No-GR and GR scenarios.

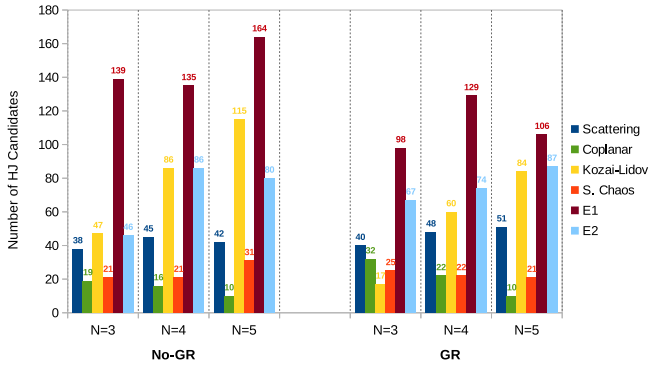

Figure 3. Statistical distribution of the number of HJ candidates produced through different high-eccentricity mechanisms as a function of the initial planet number (N) for No-GR and GR scenarios.

3.2. Efficiencies of high-eccentricity mechanisms in the production of hot Jupiter candidates as a function of the initial planetary mass configuration

We now examine how the efficiencies of high-eccentricity mechanisms in the production of HJ candidates depend on the initial planetary mass configuration. Table 3 summarizes the results derived from our investigation.

Table 3 reveals that 42.46% of the total HJ candidates produced in No-GR and GR simulations were derived from the initial equal mass configuration, which was approximately twice of the individual efficiency obtained with the initial random and increasing mass configurations. By contrast, the initial decreasing mass configuration had the lowest efficiency with 16.12% of the total HJ candidates. The high efficiency obtained with the initial equal mass configuration can be accounted to the fact that it generated initially more tightly-packed multi-planet systems, which significantly decreased the number of systems without dynamic instability events.

Table 3 also shows that the E1 mechanism was notably efficient in the HJ candidate production in the initial random, increasing, and decreasing mass configurations in both scenarios No-GR and GR. In fact, on the one hand, the efficiency of formation of HJ candidates by E1 mechanism derived from such initial planetary mass configurations ranged from $< 39\%$ and $< 51\%$, where the highest percentages are associated with the initial decreasing mass configuration. On the other hand, the efficiencies of the other high-eccentricity mechanisms resulting from the initial random, increasing, and decreasing mass configurations did not reach 22%. In the initial equal mass configuration, the efficiency of HJ candidate production from the E1 mechanism (27.99%) was slightly surpassed by the Kozai-Lidov mechanism (28.19%) in the No-GR scenario, while, in the GR simulations, the efficiency of E2 mechanism (30.24%) was more significant than that derived from the E1 mechanism (20.23%).

For comparative purposes, the most efficient high-eccentricity mechanisms obtained from the study developed by Wang et al. (2017) were Kozai-Lidov (36.6%), scattering (34.9%) and E1 (16.2%), while coplanar (7.6%), E2 (2.8%) and secular chaos (1.9%) were the least efficient in their simulations. We remark that the investigation carried out by Wang et al. (2017) did not include GR effects and it only considered the initial equal mass configuration with $\Delta K = 0.001$ for the development of their simulations. For the initial equal mass configuration and the No-GR scenario, we found as the most efficient mechanisms able to produce HJ candidates were Kozai-Lidov (28.19%), E1 (27.99%) and E2 (21.40%), while the least efficient ones were scattering (13.37%), secular chaos (6.79%) and coplanar (2.26%). We see that there are substantial differences between our results and the study carried out by Wang et al. (2017). This can be explained if we take into account that Wang et al. (2017) considered initial inclinations that obeyed Rayleigh distributions, a smaller ΔK interval for the generation of initial conditions, HJ candidates selected from the check of their orbital parameters obtained at the end of the integration, and a different procedure to classify HJ candidates as E2 mechanism. If we consider only the e vs $\Delta\varpi$ and e vs ω characteristics shown in Fig. 3 by Wang et al. (2017), then the E2 mechanism does not exceed 1% in efficiency in our simulations.

Table 3. Number of HJ candidates produced through different high-eccentricity mechanisms in No-GR and GR scenarios for different initial planetary mass configurations. The percentages were calculated with respect to the total number of HJ candidates produced in each scenario and initial planetary mass configuration.

Init. planet. mass config.	Scenario	Coplanar	Secular Chaos	Scattering	Kozai-Lidov	E2	E1	Total HJ candidates
Equal	No-GR	11	33	65	137	104	136	486
		(2.26%)	(6.79%)	(13.37%)	(28.19%)	(21.40%)	(27.99%)	
	GR	18	25	84	81	127	85	420
		(4.29%)	(5.95%)	(20.0%)	(19.29%)	(30.24%)	(20.23%)	
Random	No-GR	11	14	15	45	46	103	234
		(4.70%)	(5.98%)	(6.41%)	(19.23%)	(19.66%)	(44.02%)	
	GR	18	15	15	34	44	82	208
		(8.65%)	(7.21%)	(7.21%)	(16.35%)	(21.15%)	(39.43%)	
Increasing	No-GR	8	17	28	42	40	110	245
		(3.26%)	(6.94%)	(11.43%)	(17.14%)	(16.33%)	(44.90%)	
	GR	15	13	20	26	38	85	197
		(7.61%)	(6.60%)	(10.15%)	(13.20%)	(19.29%)	(43.15%)	
Decreasing	No-GR	15	9	17	24	22	89	176
		(8.52%)	(5.11%)	(9.66%)	(13.64%)	(12.50%)	(50.57%)	
	GR	13	15	20	20	19	81	168
		(7.74%)	(8.93%)	(11.90%)	(11.90%)	(11.31%)	(48.22%)	

4. Conclusions

We have analyzed the formation efficiency of HJ candidates from high-eccentricity mechanisms in planetary systems that undergo strong dynamical instabilities between gaseous giants. In particular, our investigation focused on the efficiencies of six different kinds of mechanisms, which are planet–planet scattering, coplanar migration, Kozai–Lidov mechanism, secular chaos, and E1 and E2 mechanisms. The present study is based on that developed by Wang et al. (2017), though there are several significant differences in the initial conditions and in the methodology of both works. In fact, we have been able to construct a more detailed model to analyze the formation of HJ candidates from high-eccentricity mechanisms, which has allowed us to strengthen our understanding concerning the dynamical evolution of planetary systems that undergo early strong instabilities around solar-type stars.

Of all mechanisms analyzed in our study, the E1 mechanism is the most efficient in producing HJ candidates both in simulations with GR and without GR, followed by Kozai-Lidov and E2 mechanisms. Since the GR has the effect of inhibiting the libration of the argument of pericenter of the HJ candidate, the Kozai-Lidov mechanism is less (more) relevant than E2 mechanism in simulations with (without) GR effects.

One of the most important analysis of our investigation was that concerning the sensitivity of the formation efficiency of HJ candidates from high-eccentricity mechanisms resulting from different initial planetary mass configurations. We found differences in the dominant mechanism that led to the HJ candidate production for the different initial planetary mass configurations. On the one hand, E1 mechanism was notably efficient in the generation of HJ candidates in the initial random, increasing, and decreasing mass configurations in No-GR and GR scenarios. On the other hand, in the initial equal mass configuration, the efficiency of HJ candidate production from the E1 mechanism was slightly surpassed by the Kozai-Lidov mechanism in the No-GR scenario, while the efficiency of E2 mechanism was more relevant than that obtained from the E1 mechanism in the GR simulations.

The obtained results allowed us to improve our understanding about the production of HJ candidates via high-eccentricity mechanisms.

Acknowledgements. We thanks to Julia Venturini and Tabaré Gallardo for providing the modified version of the Mercury code used in this work. We acknowledge the use of the Lobo Carneiro supercomputer from NACAD - Coppe, Universidade Federal do Rio de Janeiro (UFRJ). This study was financed in part by the Coordenação de Aperfeiçoamento de Pessoal de Nível Superior - Brasil (CAPES) - Finance Code 001.

References

Anderson, K. R., Lai, D., Pu, B., 2020. MNRAS, 491, 1369
Bailey, E. & Batygin, K., 2018. ApJL, 866, L2
Batygin, K., Bodenheimer, P. H., Laughlin, G. P., 2016. ApJ, 829, 114
Beaugé, C. & Nesvorný, D., 2012. ApJ, 751, 119
Bodenheimer, P., Hubickyj, O., Lissauer, J., 2000. Icarus, 143, 2
Boley, A. C., Granados Contreras, A. P., Gladman, B., 2016. ApJL, 817, L17
Coleman, G. A. L. & Nelson, R. P., 2016. MNRAS, 460, 2779
Fogg, M. J. & Nelson, R. P., 2005. A&A, 441, 791
Heller, R., 2019. A&A, 628, A42
Ivanov, P. B. & Papaloizou, J. C. B., 2004. MNRAS, 347, 437
Lee, M. H. & Peale, S. J., 2002. ApJ, 567, 596
Lin, D. N. C., Bodenheimer, P., Richardson, D. C., 1996. Nature, 380, 606
Mandell, A. M., Raymond, S. N., Sigurdsson, S., 2007. ApJ, 660, 823
Marzari, F. & Weidenschilling, S. J., 2002. Icarus, 156,570
Marzari, F. & Nagasawa, M., 2020. MNRAS, 493, 427
Nagasawa, M., Ida, S., Bessho, T., 2008. ApJ, 678, 498
Naoz, S., Farr, W. M., Lithwick, Y., Rasio, F. A., Teyssandier, J., 2011. Nature, 473, 187
Naoz, S., Farr, W. M., Rasio, F. A., 2012. ApJL, 754, L36
Ogihara, M., Kobayashi, H., Inutsuka, Shu-i., 2014. ApJ, 787, 172
Petrovich, C., 2015. ApJ, 805, 75
Poon, S. T. S., Nelson, R. P., Coleman, G. A. L., 2021. MNRAS, 505, 2500
Press, W. H., Teukolsky, S. A., Vetterling, W. T., Flannery, B. P., 1992. Numerical Recipes in Fortran (Cambridge Univ. Press)
Rasio, F. A. & Ford, E. B., 1996. Science, 274, 954
Raymond, S. N., Mandell, A. M., Sigurdsson, S., 2006. Science, 313, 1413
Teyssandier, J., Lai, D., Vick, M., 2019. MNRAS, 486, 2265
Vick, M., Lai, D., Anderson, K. R., 2019. MNRAS, 484, 5645
Wang, Y., Zhou, J.L., Gen, L. H., Meng, Z., 2017. ApJ, 848, 20
Yi-Han, W., Leigh, N. W. C., Perna, R., Shara, M. M., 2020. ApJ, 905, 136
Wu, Y. & Lithwick, Y., 2011. ApJ, 735, 109
Xue, Y., Masuda, K., Suto, Y., 2017. ApJ, 835, 204
Zanardi, M., de Elia, G. C., Di Sisto, R. P., Naoz, S., Li, G., Guilera, O. M., Brunini, A., 2017. A&A, 605, A64